

A Pulse Tube Cryocooler with 300 W Refrigeration at 80 K and an Operating Efficiency of 19% Carnot

Jalal H. Zia

Praxair, Inc.
Tonawanda, NY 14150

ABSTRACT

An electrically driven pulse tube cryocooler that produces 300 W of refrigeration at 80 K is now available from Praxair Inc. The unit reflects efforts by Praxair R&D to meet the need for higher operating efficiencies required by commercial HTS (High Temperature Superconducting) applications. A unique in-line design philosophy along with proprietary technology developed at Praxair allows losses in the regenerator and pulse tube to be minimized, thus achieving an efficiency of 19% of Carnot. A dual opposed ‘pressure wave generator’ from CFIC, Inc. supplies the acoustic power to the cold head.

Experimental results from refrigeration performance tests and load curves are presented. Praxair is working on the development of a family of units in this geometry with incremental refrigeration capacities. The intended application of these units to satisfy internal and external market needs, particularly in industrial gas liquefaction and HTS cooling is discussed. The cryocoolers have an integrated cold heat exchanger designed for forced convective cooling, condensation, and subcooling of a cryogenic fluid such as nitrogen. This allows convenient and direct integration into an HTS cooling system—for example, an HTS cable.

INTRODUCTION

In the fall of 2002 the US Department of Energy (DOE) solicited proposals from industry to develop cryocoolers to service the needs of future HTS devices.¹ Four standard cryocooler designs were suggested with sufficient variability to meet the needs of all potential applications of BSCCO and YBCO conductors. The Advanced Refrigeration Group in Praxair R&D successfully bid on two of the four cryocooler designs by proposing electrically driven pulse tube cryocoolers. The specifics of the two designs are shown in Table 1. Although the DOE support for one of the two cryocoolers eventually lapsed, Praxair, Inc. continued work on the cryocoolers, and significant progress has been made in meeting the DOE requirements.

Small pulse tube cryocoolers, offering <100 W of refrigeration at ≤ 80 K are commonly used for cooling cell phone electronics in transmission towers, infrared/night vision equipment cooling, small superconducting devices, etc. Developing larger pulse tube cryocoolers has been a challenge due to issues of streaming/non-uniform flow, acoustic power delivery and overall efficiency of the electro-acoustic transducer. There are few commercial pulse tube cryocoolers offering performance >150 W refrigeration at 77 K with reasonable Carnot efficiencies >12%.²

Table 1. DOE specifications for the HTS-3 cryocooler.

Parameter	Value
Temperature Range (K)	60 – 80 K
Capacity at Midpoint of temp. range (W)	300 W at 70 K
Capacity at Low End of temp. range (W)	210 W at 60 K
% Carnot Efficiency	25% minimum, 30% Goal
Cryocooler Availability %	99.8% minimum, 99.9% Goal
Mean Time to Repair (hrs)	4
MTBF (hrs)	17,520
Capital Cost \$ per cooling Watt at 65K	\$60 maximum, <\$40 Goal
Compressor/ Driver	Oil Free
System mass kg/Watt at 65K	0.75 maximum, <0.5 Goal

This is an area where significant progress has been made at Praxair, Inc. In 2003, this author reported on the development of a pulse tube cryocooler delivering 200 W at 77 K with 4 kW of electrical input power.³ Subsequently, a detailed analysis of the loss mechanisms and inefficiencies in the 200 W design was performed. The cold head was completely redesigned in an effort to increase the overall efficiency. The result is a new pulse tube cryocooler delivering 300 W at 80 K for 4.3 kW of electrical input power. Nominally, this is equivalent to 19.2% of the maximum Carnot efficiency.

CRYOCOOLER DESIGN

Thermoacoustic Design

The design was carried out using both DeltaE and SAGE software. The redundancy in the design effort allowed both software codes to complement each other. The strength of DeltaE lies in its numerical interface where amplitudes, phases and energy flows (calculated only in the primary harmonic in one dimension) represent the output of the model. The strength of SAGE lies in its ability to calculate higher harmonics and iteratively optimize for a user defined goal (often this goal is maximum efficiency or maximum refrigeration). Nevertheless, practical experience with both codes suggests that sufficient flexibility must be allowed in the mechanical design to accommodate deviations from reality in the thermoacoustic modeling.

The design philosophy was to extract as much refrigeration out of an available 3300 W acoustic wave produced by the CFIC 2S241W pressure wave generator at 60 Hz. One of the decisions made at this point was to lower the acoustic ‘power density’ in the cryocooler cross-section by increasing the area/diameter of the shell. This lowers the oscillating velocity amplitude and thus the tendency for local jetting, which can be a loss mechanism in the regenerator.

The function of the regenerator, as stated by Radebaugh et. al.⁴, is to transmit a given acoustic power from the compressor (pressure wave generator – PWG) to the cold end of the regenerator with a minimum of losses. Acoustic power in the acoustic approximation is given by the following expression:

$$\dot{E}_2 = \frac{1}{2} |P_1| |U_1| \cos \theta_{(p-U)} \quad (1)$$

where \dot{E}_2 is the acoustic power and P_1 and U_1 are the pressure amplitude and volumetric velocity amplitude respectively. $\theta_{(p-U)}$ is the local phase angle between the pressure and volumetric velocity. Therefore, in order to maximize the acoustic energy delivery at the cold end of the regenerator, the phase angle $\theta_{(p-U)}$ must be zero at the longitudinal center of the regenerator. This is in accordance with laboratory measurements by the author and with the findings of Radebaugh, et. al.⁴ Additionally, ensuring this phase relationship in the center of the regenerator also allows $|U_1|$ to be minimized for a given acoustic power flow rate. This is important because of the following relationship derived by Swift⁵

$$dP_1 = - \frac{i\omega\rho_m \frac{dx}{A} U_1}{1 - f_v} \quad (2)$$

where f_v is a spatially averaged complex function that depends on the geometry of the regenerator passages. In Eq. (2), ω is the oscillation frequency, ρ_m is the mean density of the oscillating fluid, x is distance along the oscillation axis, and A is the cross-sectional area. For typical thermoacoustic regenerators, f_v will have a small imaginary component and a real component that is ≤ 1 . In other words, in a typical regenerator, the relationship between the oscillating volumetric velocity and the pressure drop is determined by a relatively large proportionality parameter. If the volumetric velocity is not optimized to its lowest possible value (for a given acoustic energy flow) it can lead to potentially large pressure drop losses in the regenerator. Increasing the cross sectional area of the regenerator can potentially help alleviate the pressure drop; however, it raises other concerns about lateral non-uniformities not discussed in this paper.⁶

The phase angle in the regenerator can be optimized by careful tuning of the inertance length, the orifice resistance, and the compliance volume. In practice, operating the OPTR in this ‘regenerator-optimized-only’ mode rarely leads to the best refrigeration performance. Further consideration must be given to the potential for second order convective streaming inside the thermal buffer tube. This was investigated in detail by Olson and Swift.⁷ An approximate expression for eliminating streaming in a tapered thermal buffer tube was derived for helium gas at cryogenic conditions:

$$\frac{1}{A} \left(\frac{dA}{dx} \right) \approx - \frac{\omega |P_1|}{\rho_m \langle |U_1| \rangle} (0.75 \cos \theta_{p-U} + 0.64 \sin \theta_{p-U}) - 0.0058 \frac{dT_m/dx}{T_m} \quad (3)$$

One of the problems with tapered buffer tubes is they tend to be expensive to fabricate, particularly with the small taper angles required in Orifice Pulse Tube Refrigerators (OPTR’s). This drives towards making a thermal buffer tube that is a right circular cylinder. Fortunately, an important consequence of Eq. (3) is that a non-taper thermal buffer tube can be designed with zero second order convective streaming by careful management of the phase angle, θ_{p-U} , during the design process. A modified form of Eq. (3) can be included in the computer software codes during the design process to ensure a ‘streaming-neutral’ thermal buffer tube.

Another potential problem with large OPTR’s is the control of jetting at the interface of the thermal buffer tube and the inertance line. Using larger diameter inertance and a smooth transition can potentially alleviate this problem; however, a large diameter tube will need to be longer in order to provide a given inertance. Furthermore, oscillations in the core of a large diameter tube will tend to be close to adiabatic, producing a radial temperature gradient. Adiabatic gas in the core operates at a higher temperature (and lower density) than that at the periphery leading to a loss of inertance at higher power throughput. Nevertheless, the loss associated with jetting justified going to a moderately large diameter inertance tube. This also prompted the development of a proprietary flow distribution device for use at the inertance tube/cold head interface. The effectiveness of this flow distribution device can be gauged by the fact that compared to traditional screen flow straighteners, the new device provided a 6K temperature advantage for identical operating conditions of the OPTR.

Mechanical Design

Praxair, Inc. has significant prior experience with in-line OPTR's. In such a design, the regenerator, cold heat exchanger, thermal buffer tube, and both ambient heat exchangers share the same axis. Refrigeration is delivered by circulating a liquid cryogen stream through the cold heat exchanger. This particular configuration is less prone to losses associated with flow transitions and lends itself well to integration in HTS devices that require a forced/convective flow of a cryogen through them.

The cold head consists of a 'matching volume' between the aftercooler and the PWG. This is to allow acoustic impedance matching between the cold head and the PWG. All heat exchangers are shell-and-tube type with an average open area of 10%. The tube-side is for oscillatory helium while the shell-side is for the process fluid or coolant. Some heat exchangers also have multiple passages on the shell-side in order to get heat transfer enhancement especially with a condensing and/or subcooling cryogenic fluid.

The regenerator is made of layers of lightly bonded stainless steel screens of two different types. Significant time and effort has been spent on ensuring a consistent and repeatable fabrication process for the regenerator material. The porosity and layering procedure of the regenerator has to be tightly controlled in order to get optimum performance from the OPTR.

The cold heat exchanger and the ambient heat exchanger above the thermal buffer tube are of the shell & tube type. The resulting jetting into the buffer tube is controlled by layers of standard screen material at both ends. The thermal buffer tube itself is a right circular cylinder (no taper) with the phase carefully controlled to ensure zero-streaming. A variable orifice is created in the inertance line by using an in-line ball valve.

EXPERIMENTAL RESULTS & ANALYSIS

One key measure in quality control is to verify the acoustic properties of the regenerator. This includes measuring the complex impedance of the regenerator at various pressure wave amplitudes. In an in-line OPTR, this test can be performed by running the unit with the cold head isolated from the impedance by closing off the orifice (ball valve in this case). This step forces the unit to run off-resonance and without any phase adjustment by the inertance line or the compliance tank. Thus, the phase across the regenerator does not produce much refrigeration and the temperature gradient at steady state is negligible. In other words the physical properties of the

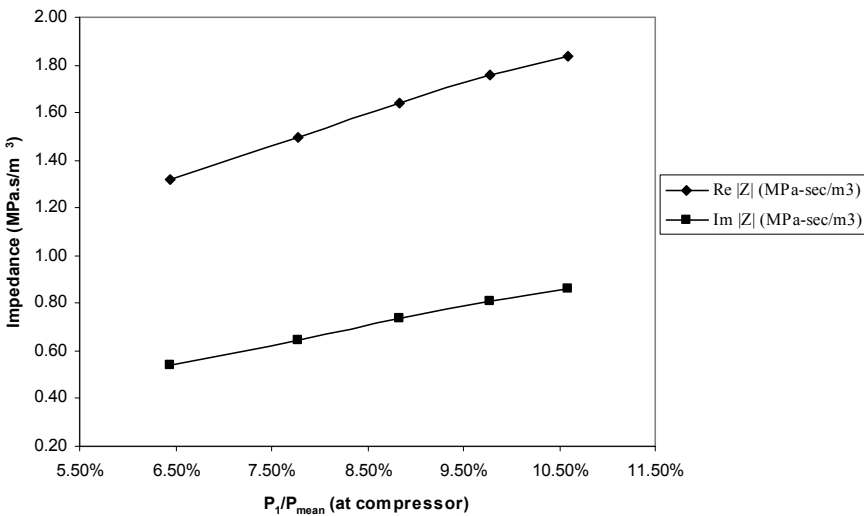


Figure 1. Complex impedance of the regenerator with varying pressure amplitudes.

charge gas (helium, in this case) can be taken as constant across and along the regenerator. Figure 1 shows the complex impedance of the regenerator measured in this manner at various pressure amplitudes. This matches well SAGE and DeltaE models using a regenerator porosity parameter of 71.5%. This was the measured porosity of the regenerator before it was inserted into the cold head.

Radebaugh et. al.⁴ reported in their work an optimum phase angle (the angle between the oscillating pressure and oscillating volumetric flow rate) at the top of the pulse tube of 60° , controlled by the orifice, inertance, and compliance network. This results in a phase of zero degrees at the axial center of the regenerator. It is further suggested by Radebaugh et.al.⁴ that the phase at the warm end of the regenerator be maintained at -30° (volume flow rate leading the pressure) and the cold end 30° . This ‘phase symmetry’ across the regenerator for maximum performance has also been the observation of this author.⁸ However, in this particular cold head design, obtaining a symmetrical phase across the regenerator led to highly adverse streaming conditions inside the thermal buffer tube. Therefore a compromise regenerator phasing that allowed acceptable mitigation of thermal buffer tube streaming was chosen as the operating point for 80 K operation. The phasing in the entire cold head is shown in Fig. 2. It can be seen that the phase at the warm end of the regenerator is -15° , while that at the cold end is 40° . The phase at the top of the pulse tube is 67° . This phase regime allowed an acceptable level of suppression of streaming at the center of the thermal buffer tube. Clearly there is room for further design optimization in this cold head.

Refrigeration performance of the cold head is measured by the change in temperature of a nitrogen stream of a known mass flow rate flowing through the cold heat exchanger. In the purely gaseous regime, the nitrogen stream is not allowed to condense in the cold heat exchanger by keeping the flow rate high. This is due to the difficulty of measuring the liquid fraction in a cryogenic fluid, should the nitrogen start condensing. In the purely liquid regime, subcooled liquid nitrogen flows through the cold heat exchanger with insulated feed and discharge lines. The above are necessary for accurate load curve measurement. However, once the load curve is determined, the cold head may be operated in any of the de-superheating, condensing, or subcooling regimes.

The load curve already accounts for the heat transfer resistances across the cold heat exchanger and the related irreversibilities; therefore, the refrigeration reported here is the net

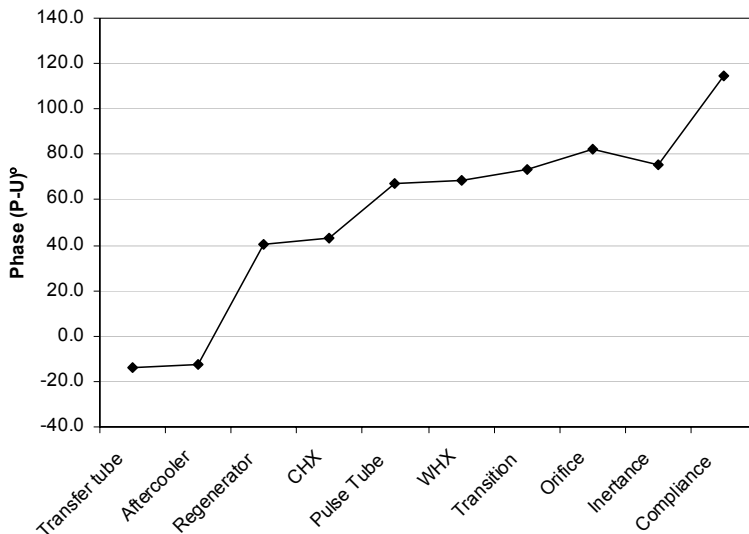


Figure 2. Phase variation in the components of the cold head while at optimum operating condition.

delivered to a stream of nitrogen. This is truly representative of the performance of the cold head when integrated into a HTS device. The resulting consolidated load curves are shown in Fig. 3. It can be seen that at 80 K (a common reference point for HTS devices and cryocoolers) the unit is able to deliver approximately 300 W of net refrigeration with 4.3 kW to total input electrical power. This leads to an overall efficiency of 19.2% of the maximum Carnot efficiency at 80 K. Figure 3 also shows another important feature that is common to all pure acoustic Stirling-type pulse tube cryocoolers: that is the ability to continuously modulate the refrigeration delivery by varying the input power without a loss of efficiency. Thus, load curves at other input electrical powers are also shown.

The cryocooler's no-load temperature was determined by placing a 4-wire RTD on the outside shell of the cold heat exchanger and allowing the unit to run unloaded to steady state. The cold heat exchanger body was filled with helium at 30 psig and sealed. This would preclude the possibility of liquid formation inside the cold HX body. The lowest no-load temperature recorded was 47 K. The no-load operating point is determined largely by the temperature gradient in the thermal buffer tube and the resultant streaming. At lower temperatures the impedance of the regenerator changes; this shifts the phase in the thermal buffer tube to a regime highly conducive to streaming. This, in addition to the steep temperature gradient across the thermal buffer tube, results in a higher than expected no-load temperature. More work towards streaming suppression at lower temperatures should result in a lower temperature; however, this is not the focus of this work at present.

CONCLUSIONS

An electrically driven pulse tube cryocooler that produces 300 W of refrigeration at 80 K has been successfully designed, tested, and operated at Praxair, Inc. The unit delivers refrigeration by de-superheating, liquefying and/or subcooling a cryogen such as nitrogen. An overall efficiency of >19% of Carnot is achieved at 80 K with 4.3 kW total input power. This is a significant milestone in meeting the requirements envisioned by the DOE for an HTS-3 class cryocooler (as shown in Table 1).

The unit is headed for field service in Praxair internal applications such as high-value cryogen conservation (argon). Beta tests with an OPTR attached to a bulk cryogenic tank have

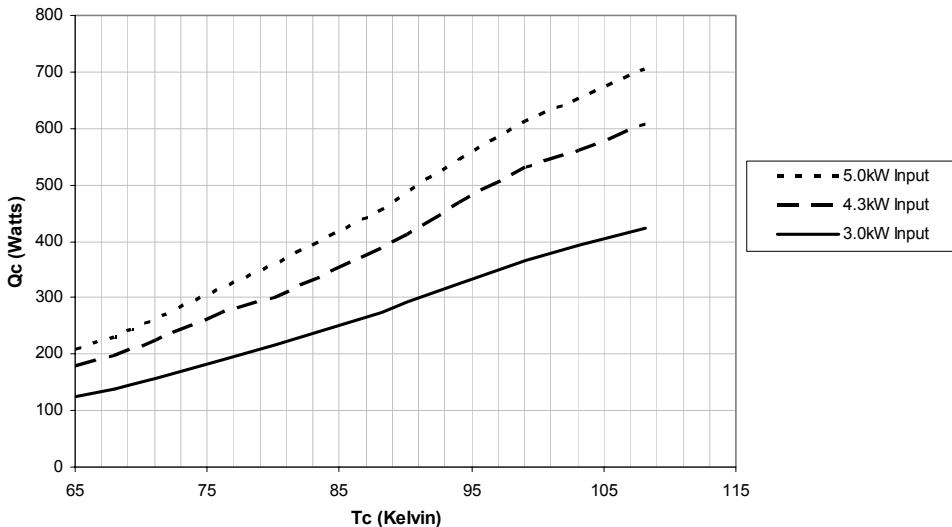


Figure 3. Load curves at several different total input power levels. The refrigeration can be continuously modulated by varying the input power.

yielded encouraging results for reducing cryogen losses from the bulk tank. In this application, the unit is typically unattended and unserviced, while operating outdoors in adverse weather conditions. Therefore, considerable progress has been made into making the unit controllable, safe, and durable for long term continuous or intermittent operation.

ACKNOWLEDGMENT

The author would like to thank Nancy Lynch (Praxair), Greg Swift (LANL), and John Corey (CFIC) for providing valuable advice and guidance in the design of the cryocooler.

REFERENCES

1. US Department of Energy/ORNL solicitation no. 6400002482 / 08/28/2002.
2. Ter Brake, H.J.M., Wiegerinck, G.F.M., "Low-power cryocooler survey," *Cryogenics*, Vol. 42, No. 11 (2002), pp.705-718.
3. Zia, J. H., "Design and Operation of a 4kW Linear Motor Driven Pulse Tube Cryocooler," *Adv. in Cryogenic Engineering*, Vol. 49B, Amer. Institute of Physics, Melville, NY (2004), pp. 1309-1317.
4. Radebaugh, R., Lewis, M., Luo, E., "Inertance Tube Optimization for Pulse Tube Refrigerators," *Adv. in Cryogenic Engineering*, Vol. 51, Amer. Institute of Physics, Melville, NY (2006), pp. 59-67.
5. Swift, G.W., "Thermoacoustics: A Unifying Perspective for Some Engines and Refrigerators," Acoustical Society of America, American Institute for Physics Press, New York (2002).
6. So, J.H., Swift, G.W. and Backhaus, S., "An Acoustic Streaming Instability within Regenerator-Based Thermoacoustic Devices," *J. Acoust. Soc. Am.*, Vol. 115 (2004), pp. 2381.
7. Olson, J.R. and Swift, G.W., "Acoustic Streaming in Pulse Tube Refrigerators: Tapered Pulse Tubes," *Cryogenics*, Vol. 37 (1997), pp. 769-776.
8. Zia; J. H., "A Commercial Pulse Tube Cryocooler with 200 W Refrigeration at 80 K," *Cryocoolers 13*, Springer Science+Business Media, New York (2005), pp. 165-171.